Compact hohlraum configuration with parallel planar-wire-array x-ray sources at the 1.7-MA Zebra generator

V. L. Kantsyrev,[1] A. S. Chuvatin,[2] L. I. Rudakov,[3] A. L. Velikovich,[4] I. K. Shrestha,[1] A. A. Esaulov,[1] A. S. Safronova,[1] V. V. Shlyaptseva,[1] G. C. Osborne,[1] A. L. Astanovitsky,[1] M. E. Weller,[1] A. Stafford,[1] K. A. Schultz,[1] M. C. Cooper,[1] M. E. Cuneo,[5] B. Jones,[5] and R. A. Vesey[5]

[1]*Physics Department, University of Nevada, Reno, Nevada 89557, USA*

[2]*Laboratorie de Physique des Plasmas, Ecole Polytechnique, 91128 Palaiseau, France*

[3]*Icarus Research, Inc., P.O. Box 30780, Bethesda, Maryland 20824-0780, USA*

[4]*Plasma Physics Division, Naval Research Laboratory, Washington, DC 20375, USA*

[5]*Sandia National Laboratories, Albuquerque, New Mexico 87110, USA*

(Received 19 June 2014; published 2 December 2014)

A compact Z-pinch x-ray hohlraum design with parallel-driven x-ray sources is experimentally demonstrated in a configuration with a central target and tailored shine shields at a 1.7-MA Zebra generator. Driving in parallel two magnetically decoupled compact double-planar-wire Z pinches has demonstrated the generation of synchronized x-ray bursts that correlated well in time with x-ray emission from a central reemission target. Good agreement between simulated and measured hohlraum radiation temperature of the central target is shown. The advantages of compact hohlraum design applications for multi-MA facilities are discussed.

DOI: 10.1103/PhysRevE.90.063101 PACS number(s): 52.58.Lq, 32.30.Rj, 52.59.Qy, 52.70.La

I. INTRODUCTION

Interest in the indirect drive of fuel capsules for inertial confinement fusion (ICF) studies has led to the development and application of the world's most powerful laser facility, the National Ignition Facility at Lawrence Livermore National Laboratory [1]. On the other hand, pulsed power offers much more efficient energy coupling than lasers [2]. In this paper, we report a proof-of-principle experimental demonstration of the full configuration of a compact hohlraum design as jointly proposed by the Sandia National Laboratories (SNL) and the University of Nevada, Reno (UNR) [3]. This design enhances efficiency over prior pulsed-power-driven concepts [2]. This approach is based on the application of multiple compact Z-pinch planar-wire-array (PWA) x-ray sources surrounding a central hohlraum cavity with a capsule or target and tailored shine shields (to provide a more symmetric temperature distribution on the capsule or target) (Fig. 1). Modeling has shown [3] that a much higher radiation temperature for a given energy input can be achieved (compared to a double-ended design [2]). The resolution of several important problems in the realization of the hohlraum design has already been achieved. The possibility of PWA x-ray pulse shaping was demonstrated [4,5], the anisotropy of PWA radiation output was studied [5], and the maximization of PWA radiation yield and power while keeping millimeter-scale source dimensions have been shown [5,6]. Recently, using a simplified compact hohlraum design (without a capsule or target and tailored shine shields), equal current redistribution in several magnetically decoupled Z-pinch PWAs driven in parallel without radiation yield and power loss was achieved [7]. The experiment was performed at the UNR 100-ns Zebra machine, in which current I was increased from 0.9 to 1.7 MA by incorporating a new load current multiplier (LCM) device [8] in the generator without changing its architecture. Zero magnetic field was observed in the central hohlraum cavity positioned between cavities with PWA sources [7]. Both latter results are important because the application of decoupled loads might lead to a loss of the magnetic insulation with unwanted discharge in the anode-cathode gap. Indeed, the preliminary analysis has shown [7] the formation of a nearly zero magnetic field region between two vertical electrode stalks at the top of the cathode directly beneath a hohlraum central cavity (Fig. 1).

Furthermore, use of the LCM allows us to reduce voltage between electrodes while increasing total load current [8,9]. In the present work, the risk of arcs forming at this magnetic null was mitigated by removing the central part of the cathode [7] under the nearly zero magnetic field region (Fig. 1).

II. EXPERIMENTAL AND MODELING RESULTS ON COMPACT HOHLRAUM RESEARCH ON UNIVERSITY-SCALE Z-PINCH GENERATOR

First experiments using the entire configuration of this compact hohlraum design were performed at the UNR 100-ns, 1.7-MA Zebra LCM generator with the load consisting of two magnetically decoupled Z-pinch double-planar-wire array (DPWA) x-ray sources driven in parallel. DPWA sources were used due to much better pulse shaping properties compared with single PWAs [3,4]. Figure 1 is a cutaway showing a structure of this assembled compact hohlraum configuration with a reemission target in the middle of the central cavity, two tailored shine shields, two cavities with x-ray sources, and radiation and current diagnostics.

The hohlraum design modeling that used the view-factor code VisRad (PRISM Computational Sciences [10]) shows promise in implementing experiments with this hohlraum design on the 1.7-MA Zebra LCM generator. While fully integrated rad-hydro simulations will be useful to develop a better understanding of the hohlraum physics, view-factor modeling is a valuable design tool, allowing us to iterate rapidly on experimental design and to demonstrate the feasibility of the concept for hohlraum and ICF studies on a 1–2-MA university-scale pulsed power platform. The hohlraum had inner dimensions of 28.5 × 12 × 10 mm (central cavity

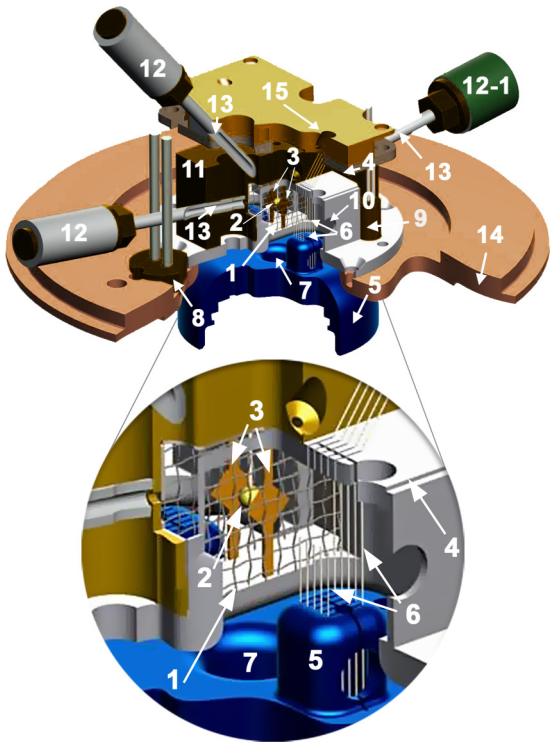

FIG. 1. (Color online) The cutaway of a compact hohlraum. 1. Central cavity with two grids at sides and four W (gold-coated) walls. 2. Reemission target in the middle of central cavity. 3. Tailored shine shields in the central cavity to provide a more symmetric temperature distribution on the reemission target. 4. One of two cavities for W DPWA sources. 5. The joint cathode with two vertical electrode stalks at the top. 6. W wires of DPWA. 7. The central hole of the cathode. 8. Micro-B-dot for total load current measurement. 9. Micro-B-dot for one of the source current measurements. 10. Diagnostics window for measuring DPWA radiation parameters. 11. EUV diode holder. 12. Filtered EUV diodes for central cavity diagnostics. 12-1. Filtered EUV diode or pinhole camera. 13. EUV collimators. 14. Anode plate. 15. Support for wire weights.

dimensions were $4.5 \times 12 \times 10$ mm). The anode-cathode gaps were 3 mm. The central cavity was separated from the source cavities by stainless steel grids with initial 70% transmission. The inner wall surfaces of each x-ray source's stainless steel cavities were coated with gold (thickness 0.2 μm) for better soft x-ray reemission. The side walls of the central cavity were made of gold-coated W plates. Two tungsten DPWA sources consist of two wire rows (5 wires in each row with interwire distance 0.7 mm) with a 3-mm inter-row gap. The W wire diameter was 7.62 μm. The central hohlraum cavity has a reemission acrylic spherical target with diameter of 1.5 mm placed in the middle of the cavity on a polyethylene holder (Fig. 1). Two concave diamond-shaped shine shields (made from stainless steel foil) were placed between the target and the sources closely to the grids' surface.

Currents were measured with calibrated micro-B-dots (PRODYN Technologies, Inc., Albuquerque, NM, USA). The current in each source cavity was measured to be at least 0.75–0.8 MA for maximum total load current $I \sim 1.65$ MA.

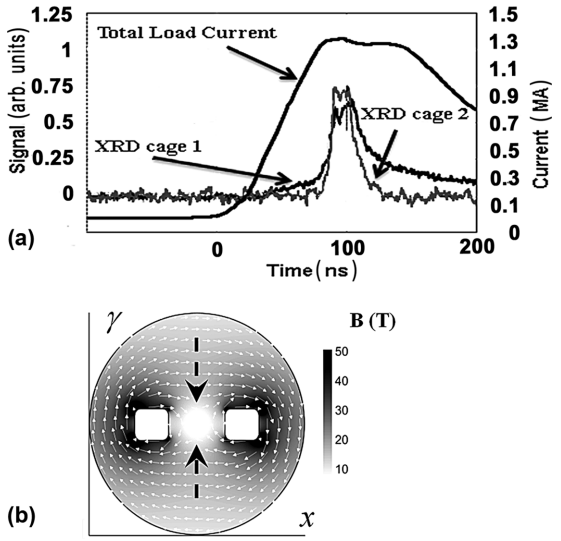

FIG. 2. (a) Comparison of XRD sub-keV signals from two cavities (cages) with W DPWA sources vs total load current. Shot no. 2798. (b) Direction and intensity B (in Tesla) of the magnetic field lines in an (X,Y) azimuthal plane positioned in the middle of the cathode-anode gap (parallel to the bottom plate of the central cavity in Fig. 1, the section through the vertical cathode stalks that connect to each DPWA). The view is from the top. Current was 1.6 MA. The region of nearly zero B is marked by arrows.

The radiation characteristics of DPWA W sources were measured with basic Zebra generator diagnostics through a hole in the end plate of the hohlraum. To reduce the effects of hole closure on the source temperature and the pinch power measurements, the size of diagnostic windows in cage walls was 2–4 mm and the distance between the plasma and the detectors was more than 1 m. Diagnostics included bare Ni bolometers (0.01–5-keV region), filtered x-ray diodes (XRDs) measuring radiation in the sub-keV region (>0.2 keV), and photoconducting detectors (PCDs) sensitive in the keV region (>0.8 keV). Only shots with a maximum x-ray peak position deviation of ± 10 ns with respect to the current maximum were selected for analysis. The average peak power in the sub-keV region (>0.2 keV) of the source in each cavity was found to be $P_{\mathrm{DPWA}} = 0.65$ TW. Driven in parallel, these Z-pinch sources showed similar simultaneous x-ray bursts with nearly equal amplitudes. The synchronized simultaneous sub-keV (>0.2-keV) x-ray bursts from cavities are shown in Fig. 2(a). The deviation of the interval between the peaks of sub-keV bursts in cavities was found to be ± 0.9 ns, which can be explained by a simulation that demonstrated the high symmetry of the magnetic field in the interelectrode gaps [Fig. 2(b)]. This together with the experimental data suggests uniform current delivery to each DPWA x-ray source and robust reproducibility of such plasma radiation sources.

The central cavity hohlraum environment was analyzed by cross-calibrated AXUVHS5 diodes (Opto Diode Corp., Newbury Park, CA, USA) with different integrated filters: Al (thickness $d = 150$ nm, cutoff energy $E_{\mathrm{cf}} = 17$ eV), Al/C ($d = 200/50$ nm, $E_{\mathrm{cf}} = 37$ eV), Si/Zr ($d = 100/200$ nm, $E_{\mathrm{cf}} = 65$ eV), or $\mathrm{Cr/Al_2}$ ($d = 100/200$ nm, $E_{\mathrm{cf}} = 300$ eV). All diodes (Fig. 1) registered radiation from a central cavity

through tungsten-carbide collimators (inner diameter 1 mm). The larger size of the collimators' opening allowed a reduction of the diagnostic hole closure effect. The two collimated EUV diodes (at the left in Fig. 1) can register radiation from only the same spot (1.1 mm diameter) on the side surface of the reemission target. The initial alignment (before placing the load in the generator chamber) was made with a He-Ne gas laser and microscope. The third calibrated, filtered EUV diode (if utilized), that observed the same spot on a opposite side of the target, was used for estimation of a nonuniformity of the target reemission in different directions. For more data, a pinhole camera or a spectrometer might be use instead of a third diode.

Experimental estimation of the reemission target surface radiation temperature T_R was performed by comparing pairs of signals from different cross-calibrated Si diodes, assuming the existence of blackbody radiation sources in the cavities. Experiments with the same type of reemission target without and with shine shields were performed for comparison. The experimental T_R of the reemission target without shine shields was around 45–55 eV (for different diode pairs) in comparison to $T_R \sim 38$ eV at the point closest to the W source, and 33 eV on the side target surface from VisRad simulations. The T_R was in reasonable correlation with VisRad modeling. The predicted nonuniformity of T_R distribution on the target surface was estimated to be about 15%. In addition, we compared the two-source scheme with a single-sided drive hohlraum (one W DPWA source with current 1.6 MA and power 1.1 TW, without tailored shine shields). In this case, the maximum T_R will be 42 eV at the point closest to the W source. But the asymmetry of the temperature distribution will be 35–38% compared with 15% in a hohlraum with two wire array sources.

The uniformity of the distribution of T_R on the target surface was improved significantly with the application of tailored shine shields between the sources and a target (Fig. 1). Also, we are taking into account that the W DPWA is an anisotropic x-ray source [5] (typical ratio $K = 1.2$ of power radiated along wire rows to one emitted orthogonal to planes was measured in our Zebra tests), and maximum radiation is emitted in the direction parallel to the wire planes [5]. In this particular scheme a proper design of shine shields was applied to use the anisotropy to increase the radiation flux at the target surface. Modeling with a modified VisRad showed that T_R will be 35.3 eV at the point closest to the shield and 38.7 eV on the side target surface. The maximum nonuniformity of the T_R distribution on the target surface in the scheme with tailored shine shields was estimated to be 9%.

Altogether there were four experiments with a full configuration with central target and tailored shine shields. Diode signals were shown to have the same amplitude (Fig. 3) for illustrative purposes.

Experimental T_R of a reemission target with shine shields was measured to be $T_R = 37 \pm 3$ eV (for different diodes pairs) in comparison to $T_R \sim 38.7$ eV at a point on the side target surface in VisRad simulation. Hence, simulation shows good agreement with the results of the first experiments on a reemission target T_R measurement with the full configuration of this hohlraum design. The EUV bursts in different spectral regions from the target correlated well with sub-keV emission (XRD signal) from the DPWA sources (Fig. 3), especially in the leading edge. At the same time, the signals' trailing edges were shorter in a harder region (>37 eV) than in the softer region (>17 eV).

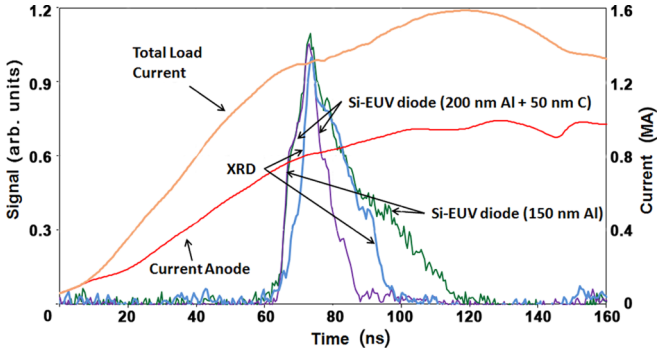

FIG. 3. (Color online) Comparison of sub-keV (XRD signal) emission from one of the W DPWA sources with EUV bursts from the acrylic reemission target in two wavelength regions (two differently filtered Si-diode signals) vs total load current and anode plate current. Shot no. 3256.

III. DISCUSSION ON POSSIBLE APPLICATION OF COMPACT HOHLRAUM CONFIGURATION AT MULTI-MA PULSED POWER FACILITIES

The results of experiments and simulations of this compact hohlraum configuration look encouraging, especially given the synchronicity and symmetry of sub-keV bursts from the sources. We might expect better symmetry of hohlraum exposure on a larger multi-MA machine just because it would be averaging over more sources in a multipinch geometry. Now that we have demonstrated the ability to field hohlraums driven by multiple pinches and the ability to model them with a view-factor code, we can confidently use this simulation tool to improve the design. The configuration of six or more pinches proposed by Chuvatin and Kantsyrev to reach better symmetry of hohlraum exposure, and shown in Fig. 4(a), seeks to do this by using DPWAs. The application of scheme Fig. 4(a), instead of the primary one [1] of Fig. 4(b) with four single planar wire arrays (SPWAs), will lead to the increase of radiation flux in the central cavity. This is made possible by the more compact DPWA (compared to the SPWA), where row planes are directed toward the central target.

In the VisRad simulation of these schemes we consider a pulsed power driver delivering on the SNL Z generator scale. The hohlraums were made of Au and the wire arrays from W; total current $I = 20$ MA ($I = 3.3$ MA at scheme A and $I = 5$ MA at scheme B in each source cavity). The basic data for W sources were average $P_{DPWA} = 0.65$ TW at $I = 0.75$ MA, SPWA power $P_{SPWA} = 12$ TW at $I = 6$ MA [1]. The current scaling of planar array source power is estimated to be $P \sim I^{1.3-1.8}$ [3,6,11]. Figures on the conservative end are $P \sim I^{1.3}$ for $P_{DPWA} = 7.5$ TW per source (six-source scheme) at $I = 3.3$ MA, and $P_{SPWA} = 10$ TW (four-source scheme) per source at $I = 5$ MA. The VisRad simulation demonstrated $T_R \sim 85$ eV (2-mm diameter target), taking into account DPWA source anisotropy $K_{DPWA} = 1.2$ for the six-source scheme, and ~80 eV for the four-source scheme

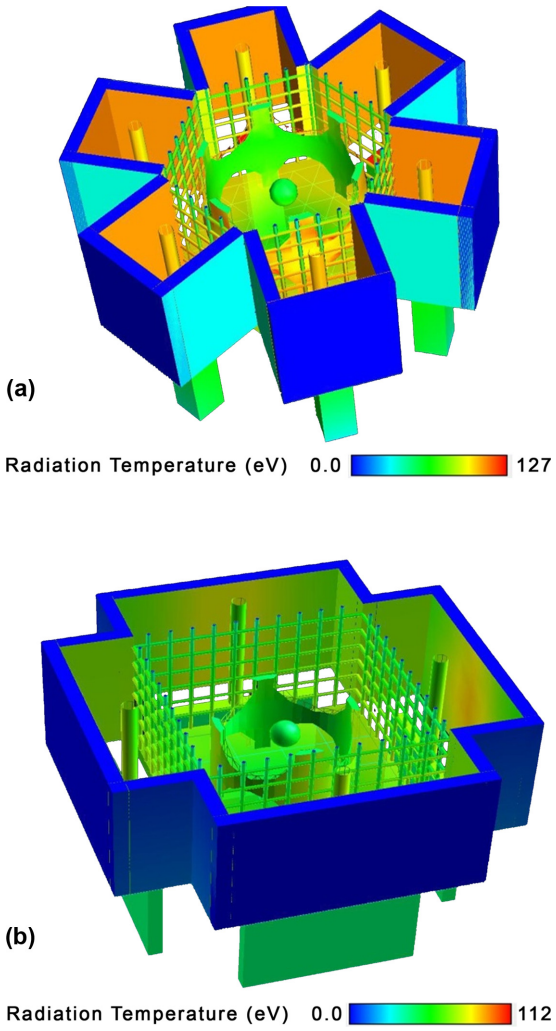

FIG. 4. (Color online) Comparison of indirect drive configurations in VisRad modeling (end-on view) with six DPWAs (a) and four SPWAs (b). The sources' plasma columns at final stagnation stage are shown together with the top cathode surfaces (top covers are not shown). The central cavities were separated from the sources by Au grids with an initial 70% transmission. The central plastic target is surrounded by similarly shaped Au tailored shine shields in both schemes. The minimal anode-cathode gap was 2 mm. (a) DPWA has initial inter-row gap $\Delta = 2.5$ mm and width $D_d = 2.5$ mm, height $H_d = 10$ mm. Each source cavity has the width $W_d = 6.5$ mm, length $L_d = 6.5$ mm, $H_d = 10$ mm. (b) SPWA has $D_s = 12$ mm, $H_s = 10$ mm. Each source cavity has $W_s = 5$ mm, $L_s = 16$ mm, $H_s = 10$ mm.

($K_{SPWA} = 1.2$). Hence, in six-source scheme, the x-ray power flux ($\sim T_R{}^4$) might be 1.3 times higher than that in the four-source one. In addition to the increase in power flux, the use of DPWA will provide the radiation pulse shaping possibility [4]. Time-dependent anisotropy [5] might also be used for effective radiation pulse shaping [4,11]. The uniformity of the T_R distribution at the target surface with shields (that have not yet optimized) was 5–7%. It can be reduced to 1.5% by optimization of shine shields shape [3].

A hohlraum scheme with parallel-driven Z pinches is a significant advance in terms of driver requirements compared to a double-ended cylindrical pinch scheme [12], because even the geometric arguments from Ref. [3] show that the scheme with parallel-driven pinches could be more efficient by a factor of ~4.5 in terms of energy requirements. Then, energy requirements directly translate to the size of the Z-pinch generator, so this would make a significant impact on size and cost of a future pulsed-power-driven ICF facility. Also, there is further opportunity for improvement and optimization of this hohlraum design. In particular, it might be useful to employ double flat-planar-foil sources instead of DPWAs [7] at currents of more than 30–50 MA, because at such current any wire arrays (cylindrical or planar) may be transformed into foils because the required diameter of wires will increase and the interwire gap will shrink. Note that the highest yields and power from the SNL Z generator were obtained with thin wire (4–5 μm diameter) loads made from W (atomic number $Z_a = 74$) [12]. Experiments on Zebra demonstrated that even more than a W load's yield and power can be obtained from a gold (Au, $Z_a = 79$) PWA [13]. VisRad simulation has shown that x-ray power flux might be ~1.3 times higher than with W in this hohlraum design with Au sources and central target [13]. Preparation of thin W flat foils is difficult because such W loads will be extremely brittle. In contrast, even submicrometer flat Au foils are very reliable and strong [7], which will be important with applications of a multisource hohlraum design due to an increase in radiation yield and power and much simpler Au foil load preparation compared with W.

IV. CONCLUSION

In summary, a proof-of-principle experimental demonstration of the full configuration of a compact hohlraum design with parallel-driven Z-pinch sources, central reemission target, and tailored shine shields (to provide a symmetric temperature distribution on the target) was achieved. The results and a code that is validated by experiments point to further studies enhancing the hohlraum design and addressing hohlraum physics. The present data demonstrate that multi-Z-pinch hohlraum configurations are realizable. Numerical simulation shows good agreement with the measured radiation temperature of the reemission target at around 30–40 eV and demonstrates the possibility of applying a multisource compact hohlraum design for multi-MA ICF review experiments.

ACKNOWLEDGMENTS

This work was supported by the DOE/NNSA under Cooperative Agreements No. DE-NA0001984 and No. DE-FC52-06NA27586, and in part by Agreement No. DE-NA0002075 and a DOE/SNL Grant No. 681371. Sandia National Laboratories is a multiprogram laboratory managed and operated by Sandia Corporation, a wholly owned subsidiary of Lockheed Martin Corporation, for the U.S. Department of Energy's National Nuclear Security Administration under Contract No. DE-AC04-94AL8500.

[1] J. Lindl, O. Landen, J. Edwards, E. Moses, J. Adams, P. A. Amendt, N. Antipa, P. A. Arnold, R. C. Ashabranner, L. J. Atherton *et al.*, Phys. Plasmas **21**, 020501 (2014).

[2] J. H. Hammer, M. Tabak, S. C. Wilks, J. D. Lindl, D. S. Bailey, P. W. Rambo, A. Toor, G. B. Zimmerman, and J. L. Porter Jr., Phys. Plasmas **6**, 2129 (1999).

[3] B. Jones, D. J. Ampleford, R. A. Vesey, M. E. Cuneo, C. A. Coverdale, E. M. Waisman, M. C. Jones, W. E. Fowler, W. A. Stygar, J. D. Serrano *et al.*, Phys. Rev. Lett. **104**, 125001 (2010).

[4] V. L. Kantsyrev, A. S. Safronova, A. A. Esaulov, K. M. Williamson, I. Shrestha, G. C. Osborne, M. E. Weller, M. F. Yilmaz, N. D. Ouart, V. V. Shlyaptseva *et al.*, J. Phys.: Conf. Ser. **244**, 032030 (2010).

[5] V. L. Kantsyrev, A. S. Chuvatin, A. A. Esaulov, A. S. Safronova, L. I. Rudakov, A. Velikovich, K. M. Williamson, G. C. Osborne, I. K. Shrestha, M. E. Weller *et al.*, Phys. Plasmas **20**, 070702 (2013).

[6] V. L. Kantsyrev, A. S. Safronova, A. A. Esaulov, K. M. Williamson, I. Shrestha, F. Yilmaz, G. C. Osborne, M. E. Weller, N. D. Ouart, V. V. Shlyaptseva *et al.*, High Energy Density Phys. **5**, 115 (2009).

[7] V. L. Kantsyrev, A. S. Chuvatin, A. S. Safronova, L. I. Rudakov, A. A. Esaulov, A. L. Velikovich, I. Shrestha, A. Astanovitsky, G. C. Osborne, V. V. Shlyaptseva *et al.*, Phys. Plasmas **21**, 031204 (2014).

[8] A. S. Chuvatin, V. L. Kantsyrev, L. I. Rudakov, M. E. Cuneo, A. L. Astanovitskiy, R. Presura, A. S. Safronova, W. Cline, K. M. Williamson, I. Shrestha *et al.*, Phys. Rev. Spec. Top.–Accel. Beams **13**, 010401 (2010).

[9] A. S. Chuvatin, V. L. Kantsyrev, A. L. Astanovitsky, R. Presura, A. S. Safronova, B. Le Galloudec, V. Nalajala, K. Williamson, I. Shrestha, G. Osborne *et al.*, in *Proceedings of the IEEE Pulsed Power Conference (PPC)* (IEEE, New York, 2011), pp. 975–982.

[10] J. J. MacFarlane, J. Quant. Spectrosc. Radiat. Transfer **81**, 287 (2003).

[11] K. M. Williamson, V. L. Kantsyrev, A. S. Safronova, A. A. Esaulov, I. Shrestha, N. D. Ouart, M. F. Yilmaz, G. C. Osborne, M. E. Weller, V. Shlyaptseva *et al.*, AIP Conf. Proc. **1088**, 141 (2009); K. M. Williamson, Ph.D. Dissertation, University of Nevada, Reno, 2011.

[12] M. E. Cuneo, R. A. Vesey, J. L. Porter, Jr., G. R. Bennett, D. L. Hanson, L. E. Ruggles, W. W. Simpson, G. C. Idzorek, W. A. Stygar, J. H. Hammer *et al.*, Phys. Rev. Lett. **88**, 215004 (2002).

[13] V. V. Shlyaptseva, V. L. Kantsyrev, A. S. Safronova, A. A. Esaulov, I. Shrestha, M. E. Weller, G. C. Osborne, and S. F. Keim, Int. J. Mod. Phys.: Conf. Ser. **32**, 1460324 (2014).